The International Journal of Advanced Manufacturing Technology (2018) 96:3977–3991
https://doi.org/10.1007/s00170-018-1835-y

ORIGINAL ARTICLE

On efficient estimation strategies in monitoring of linear profiles

Abdaljbbar B. A. Dawod[1] · **Marwan Al-Momani**[1] · **Saddam Akber Abbasi**[2]

Received: 12 August 2017 / Accepted: 25 February 2018 / Published online: 17 March 2018

Abstract
A fundamental strategy to diminish variations in manufacturing process urged the practitioners to characterize the quality of a process by a relationship between the response variable and one or more explanatory variables instead of a single quality characteristic; this state is known as a profile or a function. Profile monitoring mainly aims to test the stability of this relationship. Many researches have been carried out to study the different sampling techniques in the performance of linear profile under the maximum likely hood (MLE) estimation strategy, whereas using different estimation strategy has not been discussed so far. This paper is dedicated to introduce Bayesian estimation strategies with a proposal of novel control charts for jointly monitoring the linear profile. We considered restricted and pretest estimators, besides the estimation of distrust probability under the null hypothesis. Analytical and numerical results showed that the proposed estimators outperformed the MLE method. The proposed control charts have been used to monitor the two-phase flow in the oil industry to control the relationship between the flow rate and the pressure difference between two points.

Keywords Intercept · Slope · Error variance · EWMA · Linear profiles · Restricted estimator · Pretest estimator · Average run length

1 Introduction

Statistical process control (SPC) is a bunch of techniques used to monitor and manage the special causes of variation in a manufacturing or service processes. SPC has been adopted widely in variant new applications such as medicine, business, engineering, and social sciences (cf. [1, 2]). Control charts is the most widely used SPC toolkit; it can be used for monitoring location, dispersion, coefficient of variation, intercept, slope, etc (cf. [3, 4]).

Mainly control charts are classified into memory less and memory control charts. [5] introduced Shewhart chart as a memory less chart by using the current sample information which makes it effective to detect large shifts. In contrast, [6, 7] proposed cumulative sum (CUSUM) and exponentially weighted moving average (EWMA) charts, respectively, both charts utilize past and present information of the process which makes them effective to detect small and moderate shifts. From the practical perspective, control charts consists of two parts: retrospective phase (phase I) and monitoring phase (phase II). In phase I, a dataset is collected from the targeted process under stable conditions that represents the in-control state of the process, construct the control limits, and investigate their reliability. Phase II utilizes the control limits from phase I to monitor the process in the future (cf. [8–10]).

Many studies have been carried out to improve control charts for linear profiling, for example, [3] introduced two control chart structures to monitor a semiconductor manufacturing that was formulated as a simple linear regression with known coefficients. They used multivariate T^2 chart and EWMA/Range(R) chart (i.e., EWMA chart in conjunction with R chart to monitor the mean and the variation respectively). Their charts based on the bivariate normality assumptions of the least square estimators. [11] proposed a control chart as combination of three univariate EWMA charts to monitor the intercept, slope, and the standard deviation in phase II simultaneously.

✉ Marwan Al-Momani
almomani@kfupm.edu.sa

[1] Department of Mathematics and Statistics, King Fahd University of Petroleum and Minerals, Dhahran, Saudi Arabia

[2] Department of Mathematics, Statistics and Physics, Qatar University, Doha, Qatar

[12] compared the performance of two control charts for linear profiling in phase II. Their first control charting scheme was proposed by [13] that is known as the classical calibration method to monitor the deviation from the regression line. The second one is known as the individual monitoring of linear profile parameters of [11]. Results showed that Crowder & Hamilton's method performed poorly compared to Kim's scheme. [9] proposed the use of three control chart schemes for phase II monitoring of multivariate simple linear profiles. The results revealed that their schemes were effective in detecting the shifts in the process parameters. Recently, [14] proposed a novel control chart for jointly monitoring the linear profile, location shifts in the latent continuous distribution, and the random explanatory variables. Their simulated results revealed that the proposed chart was efficient in detecting abnormalities and was robust to various latent distributions. For more details about linear profiling, the reader is referred to [3].

Finding a consistent model by using any non-sample information has a vital role in making inferences and predictions about the characteristics of a phenomena. The non-sample information is known as *uncertain prior information* (UPI), and injecting the UPIs into the estimators is known by *Bayesian statistical methods*. A family of estimation strategies that involve the use of sample information has been introduced in the literature; under particular conditions, they outperform the traditional estimators when judged by criteria such as the mean squared error and the risk of the estimators. There has been many studies in the area of the efficient estimation relying on the work of [15] that was known by the preliminary test estimator. Later on, [16] introduced an improvement for the preliminary test of Bancroft, known as shrinkage estimator or Stein-rule for multivariate normal population that dominates the usual maximum likelihood estimator under the squared error loss criterion. More details about shrinkage strategies can be found in [17].

In this paper, we will introduce more efficient estimation strategies to estimate the linear profile coefficients that will lead to quick detection of abnormal variations in these coefficients. We employ the estimation strategies introduced by [18, 19]. Our results are compared with the results of [11].

The remainder of this paper is organized as follows: Section 2 contains some assumptions, restricted and pretest estimation strategies of simple linear regression. In Section 3, properties of the proposed strategies has been discussed. We constructed the limits of the proposed control charts in Section 4. In Section 5, we evaluated the performance of our control charts. The results of an extensive simulation study have been discussed in Section 6. Section 7 represents a real-world example that assures our simulated results. In Section 8, we give some conclusions.

2 Estimation strategies of simple linear regression model

Assume that we have a set of samples that has been collected, each of size n; the observations were given in a form of explanatory variable x and response variable y as $(x_{ij}, y_{ij}), i = 1, \ldots, n$ and $j = 1, \ldots, N$, where N is the number of samples. The model for the jth sample is given by the following regression equation

$$y_{ij} = \beta_0 + \beta_1 x_i + e_{ij}, \tag{1}$$

where e is the error component associated with the response variable. β_0 is the intercept parameter, and β_1 is the slope parameter. Errors are assumed to be independently and identically normally distributed with mean zero and variance σ^2. The model can be represented in matrix form

$$\underline{\boldsymbol{y}} = \boldsymbol{X}\underline{\boldsymbol{\beta}} + \underline{\boldsymbol{e}}, \tag{2}$$

where $\underline{\boldsymbol{y}}$ is $n \times 1$ vector of responses, X is an $n \times 2$ design matrix, $\underline{\beta} = (\beta_0, \beta_1)'$ and $\underline{e}$ is an $n \times 1$ vector of errors.

2.1 The MLE estimator of the intercept and the slope parameters

For the jth sample, the MLE estimator of β_0 and β_1 are given as follows:

$$\beta_{0j}^U = \bar{y}_j - \beta_{1j}^U \bar{x}_j, \quad \beta_{1j}^U = \frac{\sum_{i=1}^n (x_{ij} - \bar{x}_j) y_{ij}}{\sum_{i=1}^n (x_{ij} - \bar{x}_j)^2},$$

where $\bar{x}_j = \frac{\sum_{i=1}^n x_{ij}}{n}$ and $\bar{y}_j = \frac{\sum_{i=1}^n y_{ij}}{n}$.
β_{0j}^U and β_{1j}^U have a bivariate normal distribution with the mean and variance-covariance given as follows:

$$\boldsymbol{\mu} = \begin{bmatrix} \beta_0 \\ \beta_1 \end{bmatrix}, \quad \boldsymbol{\Sigma} = \frac{\sigma^2}{n} \begin{bmatrix} 1 + \frac{n\bar{x}_j^2}{Q} & -\frac{n\bar{x}_j}{Q} \\ -\frac{n\bar{x}_j}{Q} & \frac{n}{Q} \end{bmatrix},$$

where $\boldsymbol{Q} = \boldsymbol{x_j'x_j} - \frac{1}{n}(\boldsymbol{1_n'x_j})^2$.

σ^2 is estimated by S^2, that is given by

$$S^2 = \frac{(y - \hat{y})'(y - \hat{y})}{n - 2},$$

where $\hat{y}_j = \beta_{0j}^U + \beta_{1j}^U x_j$.

This unbiased estimator of σ^2 follows a χ^2 distribution with $(n - 2)$ degrees of freedom.

For more details about the MLE of the slope and intercept, refer to [20].

2.2 Restricted estimators

Assuming the UPI of the slope parameter is given by the following null hypothesis:

$$H_0 : \beta_1 = \beta_{10}. \tag{3}$$

Our target is to incorporate both the sample information and the UPI to estimate the slope. The likelihood ration (LRT) test statistics for testing the hypothesis using the jth sample in Eq. 3 is given by

$$\mathcal{L}_j = \frac{S_{xx_j}(\beta_{1j}^U - \beta_{10})^2}{S_j^2}. \tag{4}$$

The statistic follows central F-distribution with degree of freedom $(1, n-2)$ under the null hypotheses (3), and a non-central F-distribution with $(1, n-2)$ degrees of freedom with non-centrality parameter $\frac{1}{2}\Delta^2$ under the alternative, where

$$\Delta^2 = \frac{S_{xx_j}(\beta_1 - \beta_{10})^2}{\sigma^2}.$$

Usually Δ^2 is the departure constant from the null-hypothesis.

Following [17, 18], the restricted estimator of β_1 denoted by $\beta_{1j}^R(d)$ is defined by

$$\beta_{1j}^R(d) = d\beta_{1j}^U + (1-d)\beta_{10}. \quad 0 \le d \le 1, \tag{5}$$

where d is the degree of distrust in the hypothesis (3). Here, $d = 0$, means there is no distrust in H_0 or $\beta_{1j}^R(d=0) = \beta_{10}$, while $d = 1$ means there is a complete distrust in the H_0 and we get $\beta_{1j}^R(d=1) = \beta_{1j}^U$.

Similarly, we can define the restricted estimator of β_0 as follows

$$\beta_{0j}^R(d) = d\beta_{0j}^U + (1-d)(\bar{y}_j - \beta_{10}\bar{x}_j). \tag{6}$$

2.3 Preliminary test estimators

The pretest was introduced by [15], it uses the test statistics defined in Eq. 5 and the pretest estimate of the slope parameter β_1, denoted by β_{1j}^{PT} using the jth sample, and defined as

$$\beta_{1j}^{PT}(d) = \beta_{1j}^U - (1-d)(\beta_{1j}^U - \beta_{10})I(\mathcal{L}_j < F_\alpha), \tag{7}$$

where F_α is a one-sided $(1-\alpha)$-level critical value from F-distribution with $(1, n-2)$ degrees of freedom. I(A) is an indicator function of a set A.

The pretest estimator of β_0 is defined by

$$\beta_{0j}^R(d) = \beta_{0j}^U + \beta_{1j}^U\bar{x}_j(1-d)I(\mathcal{L}_j < F_\alpha) \tag{8}$$

For the proofs about these formulas, the reader is referred to [17, 18].

2.4 Estimator of residuals

Following [3, 11], to extract the residuals of a simple linear regression model at the jth sample can be achieved by the following formula:

$$\hat{e}_{ij} = y_{ij} - \hat{y}_{ij}, \quad \hat{y}_{ij} = \beta_{0j}^* + \beta_{1j}^* x_i, \quad i = 1, \ldots, n$$

where $\beta_{0j}^* \in \{\beta_{0j}^U, \beta_{0j}^R, \beta_{0j}^{PT}\}$ and $\beta_{1j}^* \in \{\beta_{1j}^U, \beta_{1j}^R, \beta_{1j}^{PT}\}$.

The average of the residuals at the jth sample can be formulated as follows:

$$\bar{e_j} = \frac{\sum_{i=1}^n \hat{e}_{ij}}{n},$$

Residuals are independent and normally distributed random variables with mean equal zero and variance σ^2, where σ^2 is estimated by

$$\text{MSE}_j = \frac{\sum_{i=1}^n \hat{e}_{ij}^2}{n-2}. \tag{9}$$

MSE_j is unbiased estimator for σ^2. In literature, the natural log of MSE_j is used more than MSE_j; hence, we will use $ln(\text{MSE}_j)$ as a measure of error variance. An approximation of the variance of $ln(\text{MSE}_j)$ due to [13] is given by

$$\text{Var}(ln(\text{MSE}_j)) \approx \frac{2}{n-2} + \frac{2}{(n-2)^2} + \frac{4}{3(n-2)^3} - \frac{16}{15(n-2)^5}.$$

For more details about the error variance, the reader is referred to [3, 11, 13].

3 Some properties of the introduced strategies

$\beta_{1j}^R(d)$ is normally distributed with mean (μ) and variance (σ_{1j}^{2R}) given as

$$\begin{aligned}\mu &= d\beta_1 + (1-d)\beta_{10}\\ \sigma_{1j}^{2R} &= \frac{\sigma^2}{S_{xx_j}}[d^2 + (1-d)^2\Delta^2] + [\frac{\sigma}{\sqrt{S_{xx_j}}}(1-d)\Delta]^2.\end{aligned}$$

The biasness (B) and *mean squared error* (MSE) based on the jth sample are given as follows:

$$\begin{aligned}B(\beta_{1j}^R) &= -\frac{\sigma}{\sqrt{S_{xx_j}}}(1-d)\Delta\\ MSE(\beta_{1j}^R) &= \frac{\sigma^2}{S_{xx_j}}[d^2 + (1-d)^2\Delta^2]\end{aligned}$$

Also, the restricted estimator $\beta_{0j}^{R}(d)$ is normally distributed with mean (μ_0^R) and variance (σ_{0j}^{2R}) given by

$$\begin{aligned}\mu_0^R &= \beta_0 + (1-d)\beta_1\bar{x}_j.\\ \sigma_{0j}^{2R} &= \sigma^2\left\{d^2\{\frac{1}{n}+\frac{\bar{x}_j^2}{S_{xx_j}}\}+(1-d)^2\frac{\bar{x}_j\Delta^2}{S_{xx_j}}\right\}\\ &\quad -[\frac{\bar{x}_j\sigma}{\sqrt{S_{xx_j}}}(1-d)\Delta]^2.\end{aligned}$$

As a result, the biasness and MSE of $\beta_{0j}^{R}(d)$ are given as

$$\begin{aligned}B(\beta_{0j}^{R}(d)) &= \frac{\bar{x}_j\sigma}{\sqrt{S_{xx_j}}}(1-d)\Delta.\\ \text{MSE}(\beta_{0j}^{R}(d)) &= \sigma^2\left\{d^2\{\frac{1}{n}+\frac{\bar{x}_j^2}{S_{xx_j}}\}+(1-\right.\\ &\quad \left.d)^2\frac{\bar{x}_j\Delta^2}{S_{xx_j}}\right\}.\end{aligned}$$

The mean, the biasness, and MSE of $\beta_{1j}^{PT}(d)$ are given by

$$\begin{aligned}E(\beta_{1j}^{PT}(d)) &= E(\beta_{1j}^{U}) - (1-d)E\Big[(\beta_{1j}^{U}-\\ &\quad \beta_{10})I(\mathcal{L}_j < F_\alpha)\Big]\end{aligned}$$

$$\begin{aligned}&= \beta_1 - (1-d)\frac{\sigma}{\sqrt{S_{xx_j}}}E\Big(\frac{\sqrt{S_{xx_j}}(\beta_{1j}^{U}-\beta_{10})}{\sigma}\\ &I(\frac{S_{xx_j}(\beta_{1j}^{U}-\beta_{10})^2}{S_{nj}^2} < F_\alpha)\Big)\end{aligned}$$

$$B(\beta_{1j}^{PT}(d)) = -(1-d)(\beta_1-\beta_{10})G_{3,n-2}(\frac{1}{3}F_\alpha;\Delta^2)$$

$$\begin{aligned}MSE(\beta_{1j}^{PT}(d)) &= \frac{\sigma^2}{S_{xx_j}}\Big[1-(1-d)^2G_{3,n-2}(\\ &\quad \frac{1}{3}F_\alpha;\Delta^2)+(1-d)\Delta^2\Big\{\\ &\quad 2G_{3,n-2}(\frac{1}{3}F_\alpha;\Delta^2)-\\ &\quad 5G_{5,n-2}(\frac{1}{5}F_\alpha;\Delta^2)\Big\}\Big]\end{aligned}$$

where $G_{m_1,m_2}(.;\Delta^2)$ is the non-central F-distribution with (m_1, m_2) degrees of freedom and non-centrality parameter Δ^2.

The mean, the biasness, and the MSE of $\beta_{0j}^{PT}(d)$ are given below:

$$\begin{aligned}E(\beta_{0j}^{PT}(d)) &= \beta_0 + (1-d)\bar{x}_j\frac{\sigma}{\sqrt{S_{xx_j}}}\\ &\quad E\Big[\frac{\sqrt{S_{xx_j}}\beta_{1j}^{U}}{\sigma}I(\frac{\sqrt{S_{xx_j}}\beta_{1j}^{U}{}^2}{S_{nj}^2}\\ &\quad < F_\alpha)\Big].\\ B(\beta_{0j}^{PT}(d)) &= (1-d)\bar{x}\beta_1G_{3,n-2}(\frac{1}{3}F_\alpha,\Delta^2).\end{aligned}$$

$$\begin{aligned}\text{MSE}(\beta_{0j}^{PT}(d)) &= \sigma^2\{\frac{1}{n}+\frac{\bar{x}_j^2}{S_{xx_j}}\}+(1-d)^2\bar{x}_j^2\\ &\quad E(\beta_{1j}^{U}{}^2I(\mathcal{L}_j < F_\alpha))+2\bar{x}_j\\ &\quad (1-d)E(\beta_{1j}^{U}(\beta_{0j}^{U}-\beta_0)\\ &\quad I(\mathcal{L}_j < F_\alpha))\end{aligned}$$

Proofs of the results besides the joint distributions are available in [17–19].

Usually, we use the mean-squared relative efficiency (MRE) to compare the MSE of our estimators with respect to the MLE; it is the ratio of the MSE for the MLE estimator to the MSE of the new estimator.

The MRE of these biased estimators depends on the departure constant Δ^2 and the degree of distrust d. Different cases are reported below:

- The MRE of β_{0j}^{R} compared to β_{0j}^{U} is

$$\text{MRE}(\beta_{0j}^{R}(d):\beta_{0j}^{U}) = A[d^2A+(1-d)^2\frac{\bar{x}^2}{S_{xx}}\Delta^2]^{-1} \tag{10}$$

  where $A = \{\frac{1}{n}+\frac{\bar{x}^2}{S_{xx}}\}$. The function takes its highest possible value at $\Delta^2 = 0$ for $d = 0$. As Δ^2 increases, the MRE decreases for all d. For some moderate to large value of Δ^2, it approaches to 0. For $d = 1$, the β_{0j}^{R} and β_{0j}^{U} are equally efficient regardless of the value of Δ^2.
- The MRE of β_{0j}^{PT} compared to β_{0j}^{U} is

$$\text{MRE}(\beta_{0j}^{PT}(d):\beta_{0j}^{U}) = A[A+\frac{\bar{x}^2\sigma^2}{S_{xx}}g(\Delta^2)]^{-1} \tag{11}$$

  where A is defined in Eq. 10,

$$\begin{aligned}g(\Delta^2) &= \Delta^2\{2(1-d)G_{3,v}(\frac{1}{3}F_\alpha;\Delta^2)\\ &\quad -(1-d^2)G_{5,v}(\frac{1}{5}F_\alpha;\Delta^2)\}-\\ &\quad (1-d^2)G_{3,v}(\frac{1}{3}F_\alpha;\Delta^2)\end{aligned} \tag{12}$$

For any d, the maximum value for the MRE attains at $\Delta^2 = 0$. As d grows larger, the MRE decreases.

- The MRE of β_{1j}^R compared to β_{1j}^U is

$$\mathrm{MRE}(\beta_{1j}^R(d) : \beta_{1j}^U) = [1 + (1 - d^2)^2\Delta^2]^{-1} \tag{13}$$

If $\Delta^2 = 0$, β_{1j}^R is more efficient than β_{1j}^U. If $\Delta^2 > 0$, the MRE depends on the value of d. For example, if $d = \frac{1}{2}$ the interval in which β_{1j}^R is more efficient than β_{1j}^U is [0, 3), while β_{1j}^U is more efficient in $[3, \infty)$ than β_{1j}^R. For $d = 0.5$, the maximum efficiency of β_{1j}^R over β_{1j}^U is 4.

- The MRE of β_{1j}^{PT} compared to β_{1j}^U is

$$\begin{aligned}\mathrm{MRE}(\beta_{1j}^{PT}(d) : \beta_{1j}^U) = {} & [(1 - d^2)G_{3,v}(\frac{1}{3}F_\alpha; \\ & \Delta^2) + (1 - d)\Delta^2 \times \\ & \{2G_{3,v}(\frac{1}{3}F_\alpha; \Delta^2) \\ & -(1 + d)G_{5,v}(\frac{1}{5}F_\alpha; \\ & \Delta^2)\}]^{-1}\end{aligned} \tag{14}$$

The MRE of β_{1j}^{PT} to β_{1j}^U monotonically decreases to minimum for Δ^2 between $\frac{1+d}{2}$ and $\frac{1+d}{1-d}$ then after monotonically increases, to approach the unit value from below.

4 Monitoring linear profile coefficients in phase II

In this section, we will discuss the structures of control charts that can be used in the monitoring of the linear profile parameters. The slope and the intercept will be monitored in addition to the residuals.

Following [11], we eliminate the correlation between the slope and the intercept before constructing the control charts for linear profiles, that can be achieved by replacing X by $X' = (X - \bar{X})$. So that the mean of the adjusted-X is zero. After the adjustment, the model in Eq. 2 will be as

$$\underline{\boldsymbol{y}} = X'\underline{\boldsymbol{\beta}} + \underline{\boldsymbol{e}}, \tag{15}$$

where $\underline{\boldsymbol{\beta}} = (\beta_0 + \beta_1\bar{x}, \beta_1)$.

Hence, we can conduct separate control chart to monitor each parameter without any problem that might result if the estimators were correlated.

Since for each sample we have n observations, we fit the model and estimate the intercept (β_{0j}), the slope (β_{1j}), and variance of the residuals (e_j) for the jth sample

Using the MLE method. We apply the proposed estimation strategies, then we adopt EWMA control chart structure for all the three parameters.

To construct the EWMA structure for monitoring the intercept (β_0), we use the estimate of β_0 at sample j; β_{0j}^*, then compute the EWMA statistics as follows:

$$\mathrm{EWMA}[j] = \lambda\beta_{0j}^* + (1 - \lambda)\mathrm{EWMA}[j - 1], \tag{16}$$

where $0 < \lambda \leq 1$ is a smoothing constant, $\mathrm{EWMA}[0] = \beta_0$ and $j = 1, 2, \ldots$.

The out-of-control signal of monitoring the parameter is given when $\mathrm{EWMA}[j] < \mathrm{LCL}$ or $\mathrm{EWMA}[j] > \mathrm{UCL}$, where LCL and UCL are the lower and upper control limits, respectively. The values of LCL and UCL are relying on the MSE of the estimator, and are given by

$$\mathrm{LCL} = \beta_0 - L\sqrt{\frac{\mathrm{MSE}(\beta_{0j}^*)\lambda}{(2 - \lambda)n}}$$

$$\mathrm{UCL} = \beta_0 + L\sqrt{\frac{\mathrm{MSE}(\beta_{0j}^*)\lambda}{(2 - \lambda)n}},$$

where $\mathrm{MSE}(\beta_{0j}^*) \in \{\mathrm{MSE}(\beta_{0j}^U), \mathrm{MSE}(\beta_{0j}^R), \mathrm{MSE}(\beta_{0j}^{PT})\}$ and L is chosen arbitrary to give specified in-control average run length (ARL).

Similarly, to construct the EWMA structure for monitoring the slope (β_1), we use the estimate of β_1 at sample j; $\beta_{1j}^* \in \{\beta_{1j}^U, \beta_{1j}^R, \beta_{1j}^{PT}\}$, then compute the EWMA statistics as follows:

$$\mathrm{EWMA}[j] = \lambda\beta_{1j}^* + (1 - \lambda)\mathrm{EWMA}[j - 1], \tag{17}$$

where $\mathrm{EWMA}[0] = \beta_1$.

The LCL and UCL are given as follows:

$$\mathrm{LCL} = \beta_1 - L\sqrt{\frac{\mathrm{MSE}(\beta_{1j}^*)\lambda}{(2 - \lambda)n}},$$

$$\mathrm{UCL} = \beta_1 + L\sqrt{\frac{\mathrm{MSE}(\beta_{1j}^*)\lambda}{(2 - \lambda)n}}$$

Finally, to construct the EWMA structure for monitoring the error variance (σ^2), we use the estimate of σ^2 at sample j; MSE_j, then compute the EWMA statistics as follows:

$$\begin{aligned}\mathrm{EWMA}[j] = {} & \max\{\lambda ln(\mathrm{MSE}_j) + (1 - \\ & \lambda)\mathrm{EWMA}[j - 1], ln(\sigma_0^2)\},\end{aligned}$$

where $\mathrm{EWMA}[0] = ln(\sigma_0^2)$.

It is more significant to detect the increases in the error variance; therefore, we well focus on UCL; for example, see [11, 21]. UCL uses the MSE of $ln(\mathrm{MSE}_j)$ as defined in Eq. 10 that is given by

$$\mathrm{UCL} = L\sqrt{\frac{\mathrm{Var}(ln(\mathrm{MSE}_j))\lambda}{(2 - \lambda)n}}.$$

As we adopted the EWMA control chart structure, we will come up with two proposed control charts that are as follows:

1. $EWMA_R$: this control chart will use the EWMA structure with the restricted estimators.
2. $EWMA_{PT}$: this control chart will use the EWMA structure with the pretest estimators.

The analytical results in Section 3 showed different behaviors with respect to their performance under the MRE. None of the estimators is found to be uniformly dominating the others.

Under H_0, β_{0j}^R, and β_{1j}^R are better choices than β_{0j}^U and β_{1j}^U because they produce higher MRE, in contrast, as we go far from H_0, the MRE of β_{0j}^R and β_{1j}^R is decreasing drastically to zero. As β_{0j}^{PT} and β_{1j}^{PT} are binary combinations of $\{\beta_{0j}^U, \beta_{0j}^R\}$ and $\{\beta_{1j}^U, \beta_{1j}^R\}$ respectively, their MRE will lay between those combinations.

From the general structure of our adopted control chart (EWMA) as it relies on the standard deviation (mean-squared error) of the estimator, the proposed estimators are supposed to excel the MLE by having smaller width of their control charts and that will play a role for early detecting the unnatural shifts in the linear relation of the monitored process.

5 Performance evaluation of charts in phase II

In this section, we compare and contrast the efficiency of our proposed control charts in phase II against the control charts that were proposed by [11]; we compare the performance in term of ARL. We adopted the same example used in their simulation study.

We will use the underlying in-control linear profile model used by [3, 11]. The model is given by

$$Y_{ij} = 3 + 2X_i + e_{ij}, \tag{18}$$

where $\beta_0 = 3$, $\beta_1 = 2$, and e_{ij} are i.i.d. normally distributed random variables with mean zero and variance one. X_i where taken arbitrary for the purpose of comparison with the previous proposed methods, as $X_i = \{2, 4, 6, 8\}$.

As we mentioned in the previous section, we start by adjusting the values of the explanatory variable. So, $X_i' = \{-3, -1, 1, 3\}$ with $\bar{x} = 0$, the model is represented as

$$Y_{ij} = 13 + 2X_i' + e_{ij}, \tag{19}$$

As our proposed estimators are biased estimators, following [10], the biasness should be removed. To set up the control limits for the unrestricted estimator, we followed [11], as they chose L for each control chart separately in order to get the in-control ARL(ARL_0) = 584. As a result, they got the joint $ARL_0 = 200$ for the simultaneous monitoring for all the parameters. The values of L as reported by [11] are given as the following: intercept (β_0^U), $L = 3.0156$, the slope (β_1^U), $L = 3.0109$, and for the error variance (MSE), $L = 1.3723$.

Following the same methodology with the new estimation strategies, we choose L that will give $ARL_0 = 200$ under the simultaneous monitoring. Some values of the constant L for some cases are given in Table 1.

Ten thousand replications have been used in our simulation study to estimate each ARL that will assure for getting stable results. In our simulation, we considered four different types of shifts. We started by introducing shifts into the intercept (β_0), slope (β_1), and the error variance; besides that, we introduced negative shifts into the slope. Similarly to [11], the description of these shifts is given as follows:

1. Shifts for the intercept δ = (0.2, 0.4, 0.6, 0.8, 1.0, 1.2, 1.4, 1.6, 1.8, 2.0) in model (19),
2. Shifts for the slope β=(0.025, 0.050, 0.075, 0.100, 0.125, 0.150, 0.175, 0.200, 0.225, 0.250) in model (18),
3. Shifts for error variance γ=(1.2, 1.4, 1.6, 1.8, 2.0, 2.2, 2.4,2.6, 2.8, and 3.0) in model (18),
4. Negative shifts for the slope β=(−1, −0.9, −0.8, −0.7, −0.64, −0.5, −0.4, −0.3, −0.2) in model (19).

All our results represented in figures are based on ARL = 200.

Table 1 Control chart multiplier L to fix $ARL_0 = 200$ for $EWMA_R$ and $EWMA_{PT}$ control charts for different values of d

Chart	d Estimator	0.1	0.25	0.5	0.75	0.95
$EWMA_R$	β_0^R	3.855	4.137	3.084	3.82	3.16
	β_1^R	3.498	3.283	3.1	3.039	3.028
	MSE	1.624	1.504	1.407	1.374	1.368
	β_0^{PT}	3.8552	3.25	3.086	3.016	3.005
$EWMA_{PT}$	β_1^{PT}	3.498	4.75	3.625	3.139	3.028
	MSE	1.624	1.492	1.407	1.373	1.368

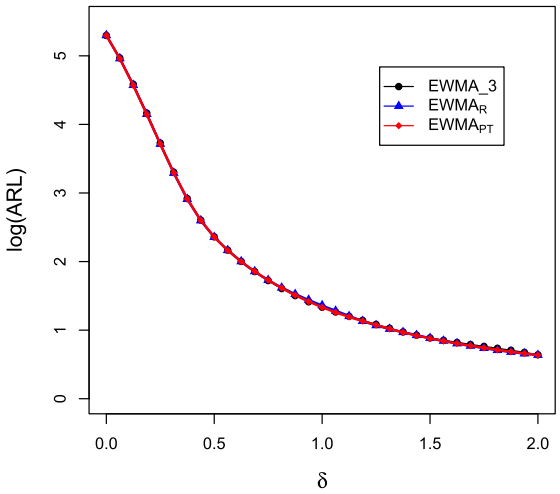

(a) Log(ARL) comparison when $d = 0.95$

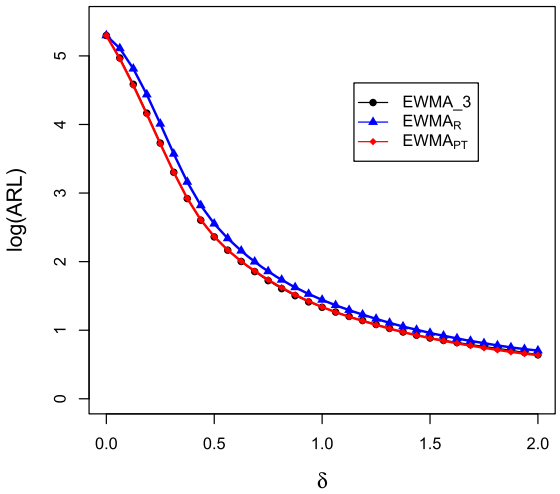

(b) Log(ARL) comparison when $d = 0.25$

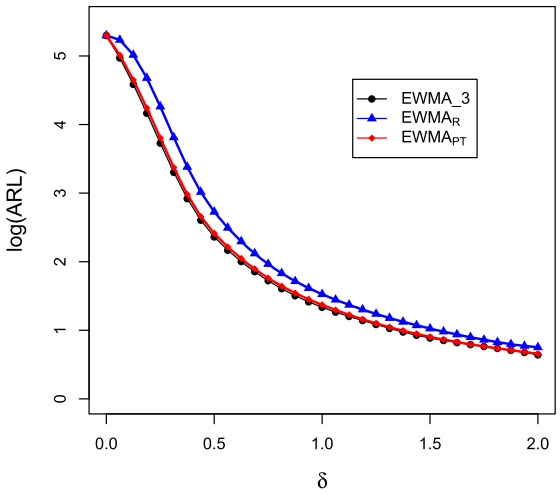

(c) Log(ARL) comparison when $d = 0.1$

Fig. 1 Log(ARL) comparisons for the intercept with shift from β_0 to $\beta_0 + \delta\sigma$. **a** $d = 0.95$. **b** $d = 0.25$. **c** $d = 0.1$

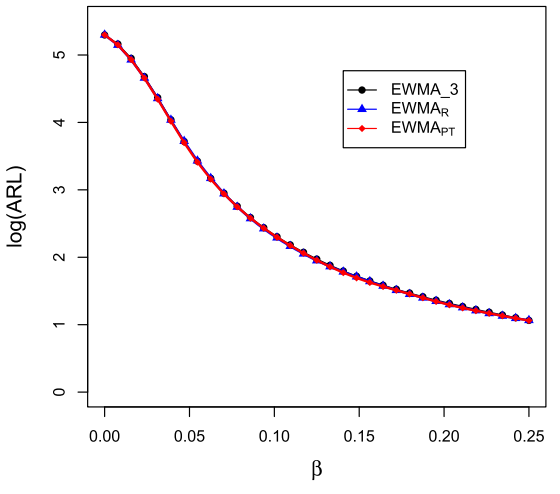

(a) Log(ARL) comparison when $d = 0.95$

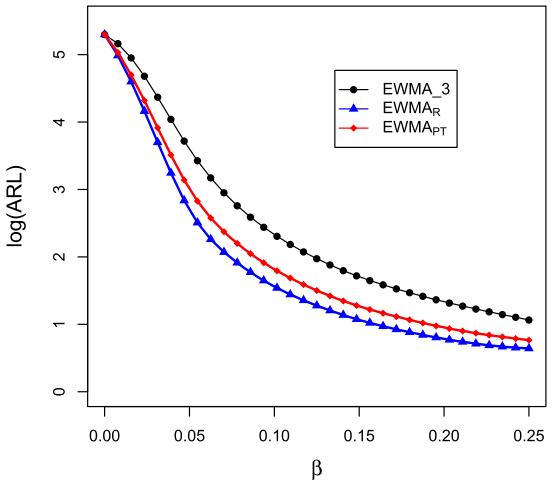

(b) Log(ARL) comparison when $d = 0.25$

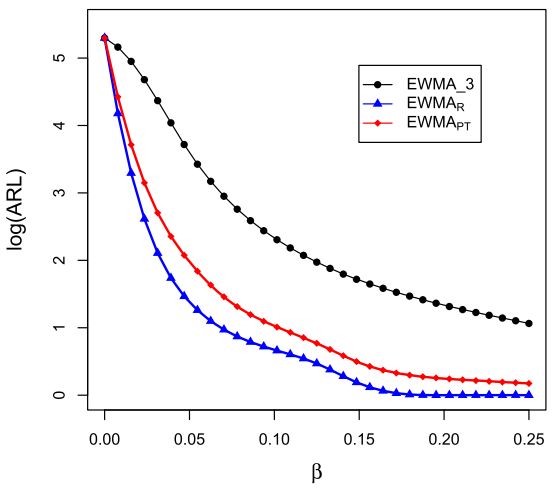

(c) Log(ARL) comparison when $d = 0.1$

Fig. 2 Log(ARL) comparisons for the slope with shifts from β_1 to $\beta_1 + \beta\sigma$. **a** $d = 0.95$. **b** $d = 0.25$. **c** $d = 0.1$

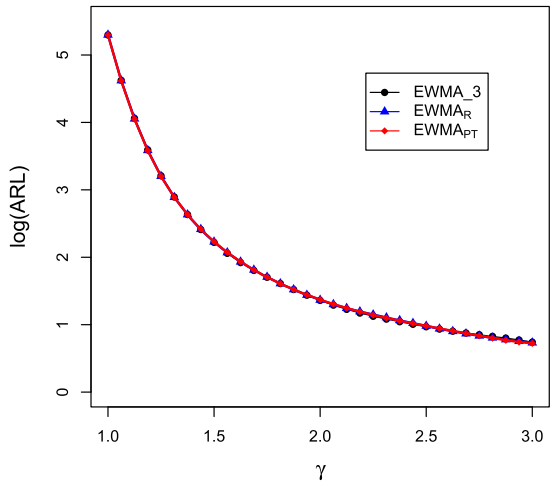

(a) Log(ARL) comparison when $d = 0.95$

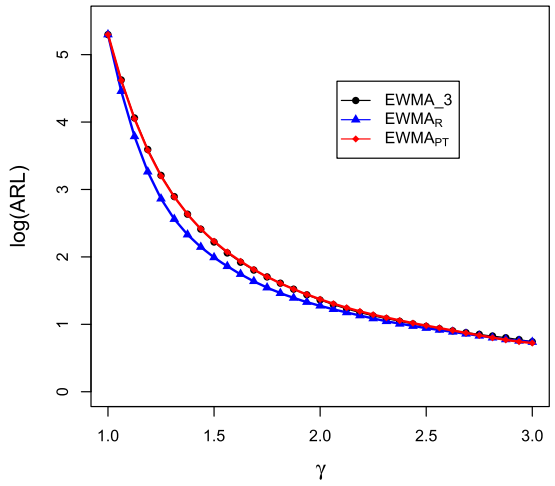

(b) Log(ARL) comparison when $d = 0.25$

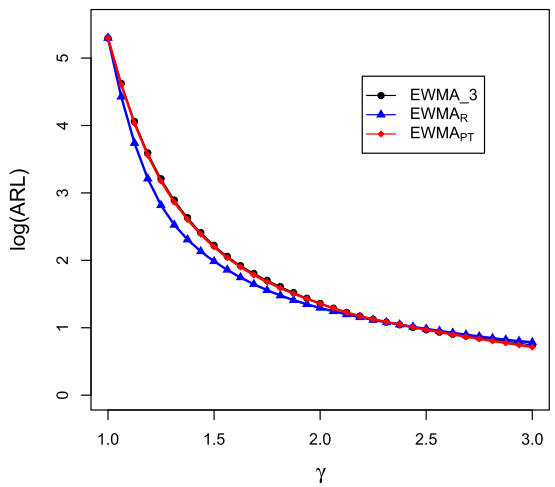

(c) Log(ARL) comparison when $d = 0.1$

Fig. 3 Log(ARL) comparisons for the error variance with shifts from σ to $\gamma\sigma$. **a** $d = 0.95$. **b** $d = 0.25$. **c** $d = 0.1$

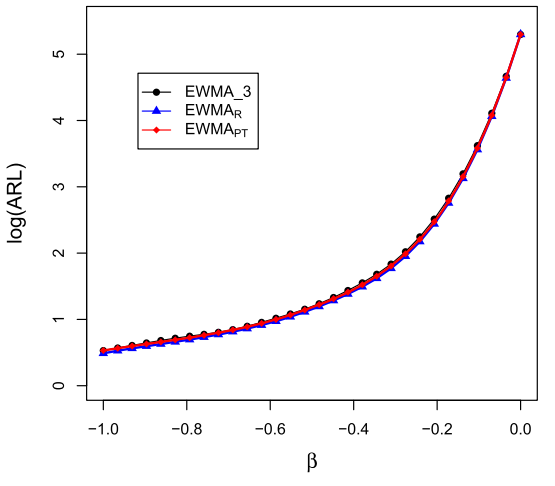

(a) Log(ARL) comparison when $d = 0.95$

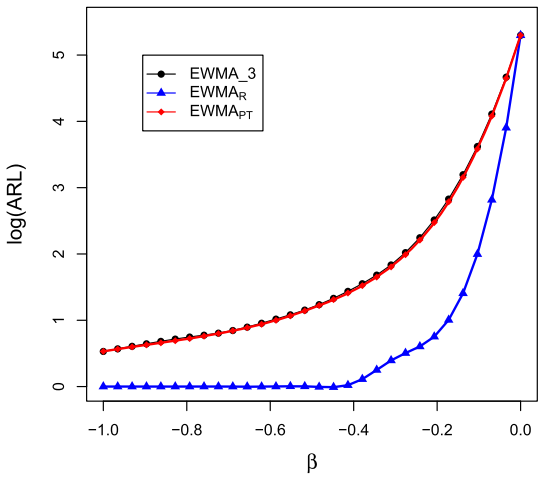

(b) Log(ARL) comparison when $d = 0.25$

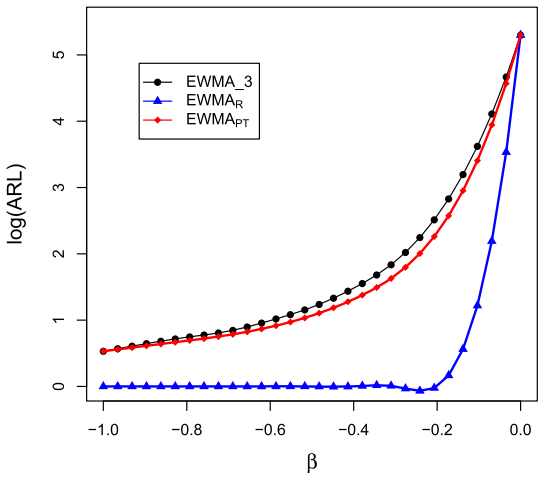

(c) Log(ARL) comparison when $d = 0.1$

Fig. 4 Log(ARL) comparisons for the slope with shifts from β_1 to $\beta_1 + \beta\sigma$. **a** $d = 0.95$. **b** $d = 0.25$. **c** $d = 0.1$

6 Discussion and comparative analysis

Here, we investigate the performance of our proposed methods and compare the results under different shifts with the results reported by [11]. All the control charts under the in-control state (the null hypothesis) have the same AR.

To study the performance of the control charts under the shifts of the intercept (β_0), the comparison is provided in Fig. 1. The different values of shifts have introduced into the intercept in terms of σ as $\beta_0 + \delta\sigma$. It is clear that the performance of our proposed methods did not excel the performance of EWMA_3; this is due to the phenomena of adjusting our explanatory variable to have a zero mean to get rid of the autocorrelation between the intercept and the slope, where $\beta_0^U = \beta^R = \beta_0^{PT} = \bar{Y}$.

As we use an approximate control limits instead of the *exact* limits of the original EWMA control chart, they slightly delay in the detection of shifts occurring with the first samples (for more details, see [22]).

Figure 2 depicts the performance of our proposed methods compared to EWMA_3 under the shifts introduced into the slope a function of σ as $\beta_1 = \delta\sigma$. The performance of our proposed methods significantly are relying on the value of the *distrust parameter (d)*. The large values of d means that we are more distrust in the null hypothesis and the performance approach toward EWMA_3 which are typically equal when $d = 1$.

Our proposed methods uniformly excel EWMA_3 with smaller values of d, where we have more trust in the null hypothesis over the entire range of shifts considered. The performance of the restricted estimator outperforms other estimators under the small amount of shifts and its performance decays with moderate and big shifts.

Figure 3 shows the ARL performance of our proposed methods compared to EWMA_3 chart for detecting out-control state in σ under a range of shifts that are expressed in terms of σ as $\gamma\sigma$. Our proposed methods outperform EWMA_3 under the small amount of shifts, whereas under the large amount of shifts, all the methods almost have the same performance. In addition, the degree of the distrust has a significant impact on the performance of the proposed methods as the methods with the smaller degree of the distrust excelled the methods with the larger degree of the distrust.

Figure 4 shows the performance of the control charts under the negative shifts in the slope. The performance of the proposed control charts under small-to-moderate shifts excels EWMA_3 as long as d decreases.

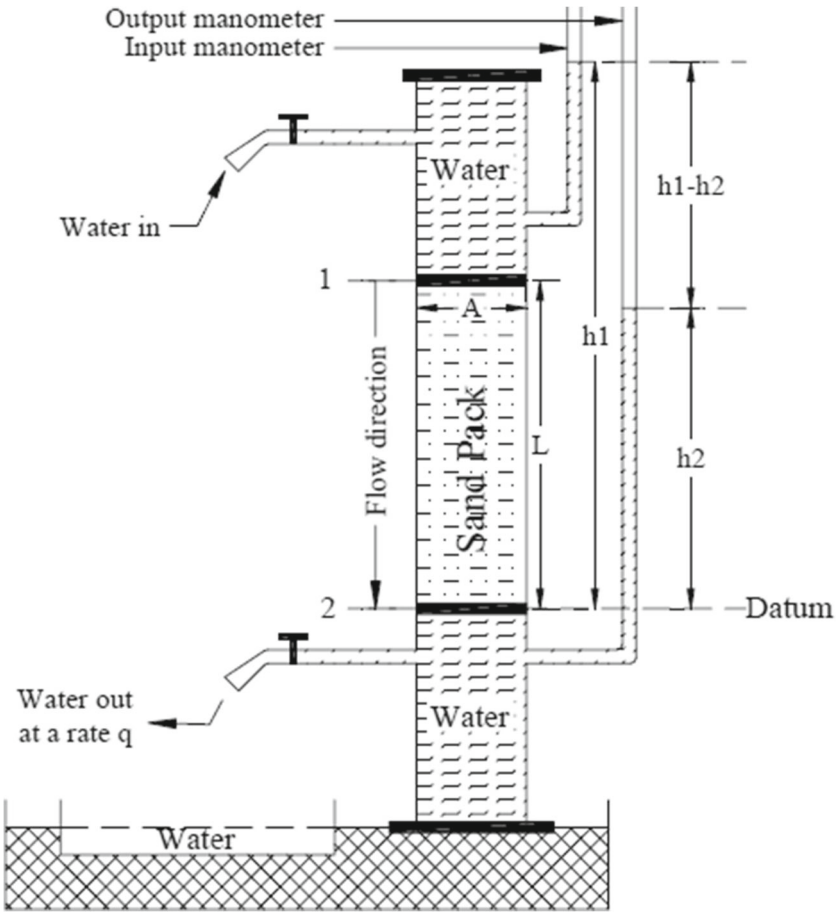

Fig. 5 Darcy law of the flow of water through sand filter

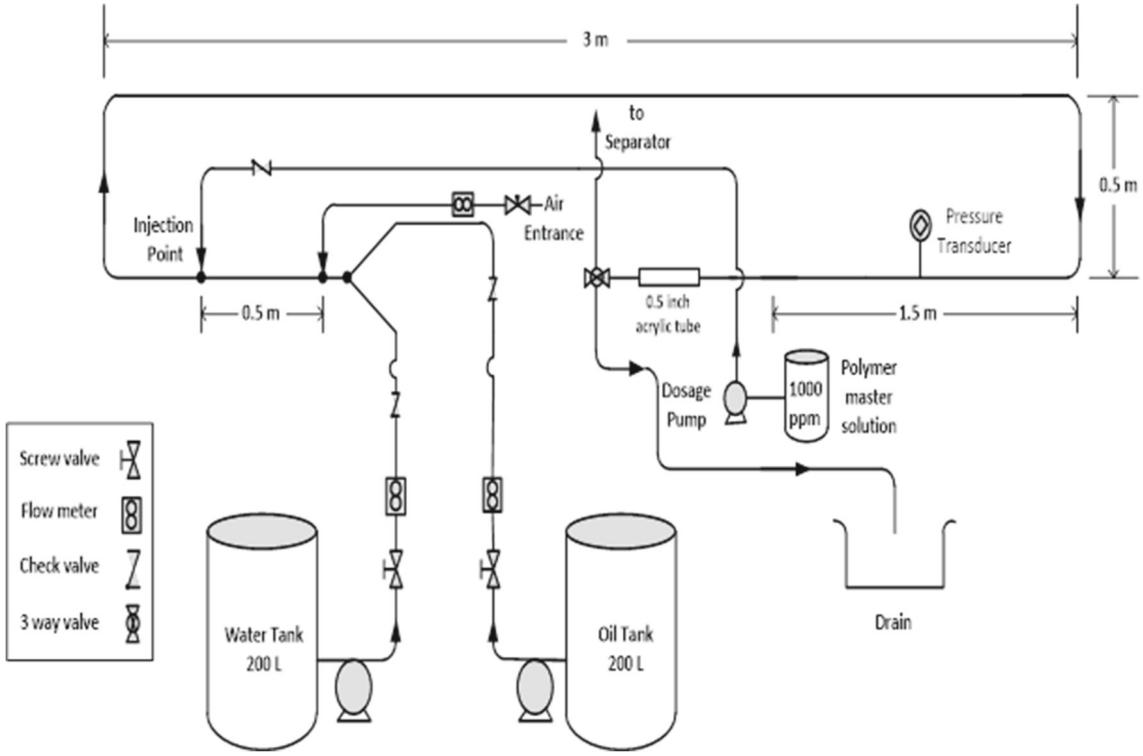

Fig. 6 Two-phase experimental setup

7 Illustrative examples

In this section, illustrations with the real-life example of linear profiles in the oil industry is discussed.

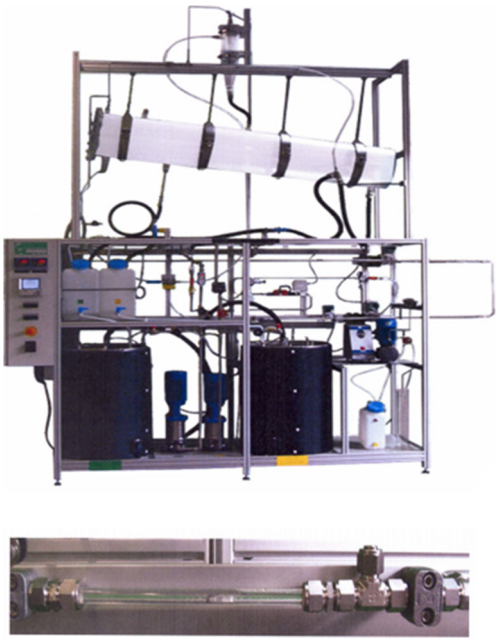

Fig. 7 Acrylic section for visual flow investigation and temperature sensor

7.1 Darcy law of single-phase flow

Very early, [23] investigated the flow of water (single-phase) through sand filter, and throughout his experiment, he concluded the following points:

- The flow rate is direct proportion to the difference of water levels in the two manometers.
- The flow rate is direct proportion to the cross-sectional area of the sand pack.

Fig. 8 Air flow rate measuring device

Fig. 9 Water flow rate measuring device

- The flow rate is inversely proportion to the length of the pack.

The water level in the manometer can be represented as the pressure head at that point, so the level difference can be replaced by the pressure difference. Figure 5 shows the experimental setup of Darcy. The outcome of Darcy experiment is summarized in the following formula:

$$q = C\frac{A}{L}(h_1 - h_2), \tag{20}$$

where q is the measured flow rate, A is the cross-sectional area, L is the Length, h is the level of water, and C is the proportionality constant.

Fig. 10 Data acquisition integrated with a software package

Table 2 The values of the constant L

	EWMA_3	$EWMA_R$	$EWMA_{PT}$
Intercept	2.997	3.137	3.009
Slope	2.992	2.973	3.005
MSE	65.897	66.32	65.91

7.2 Multiphase flow

The term of multiphase flow refers to the flow of any fluid consists of more than one phase or component with different chemical properties through a pipe or channel simultaneously. This term was coined lately by [24] and it comprises of fluid dynamics motion of multiple phases. Multiphase flow is commonly seen in industrial processes such as pipeline transportation, fluidized beds, and power plants. Liquid-liquid flows have many important applications in a diverse range of process industries in the petroleum production particularly, where oil and water are often produced and transported together. A typical multiphase oil-water two-phase flow is often encountered in petroleum industries, and measuring their process parameters (especially individual flow rate of oil and water) is an important issue in oil exploitation and transportation. Analogously in multiphase flow, probably the key toward understanding the phenomena of pressure drop behavior in oil field industries in order to optimize between the huge costs of production and transportation.

7.3 Experimental setup and data description

The experiment of two-phase flow has been conducted in the laboratories of Petroleum and Geological sciences college at King Fahd University of Petroleum and Minerals, Dhahran, Saudi Arabia. The experiment was designed to investigate the influence of some additives on the flow behavior of water, oil, and air mixture. The loop contains two 200-l barrels for water and oil respectively, besides an air connection instrument to supply the air. The flow rate of the feed streams was measured and adjusted by regulating valves.

Table 3 Control limits for each control chart

		EWMA_3	$EWMA_R$	$EWMA_{PT}$
Intercept	LCL	358.6052	358.6989	358.7782
	UCL	381.6548	381.5611	381.4818
Slope	LCL	25.3246	25.3267	24.3370
	UCL	26.8476	25.4754	26.4630
MSE	UCL	8.0148	8.0663	8.0642

The feed pumps for the liquids (oil and water) are rotary pumps equipped with axial face sealing. Water, air, and oil can be separated in the separator or using cyclone and separator which are connected to the outlet of the test section. The test section was made of stainless steel tube with an outer diameter of 0.5 in. and an inner diameter of 0.4 in. Its total length is approximately 5 m divided into two straight horizontal sections separated by elbows (90° elbow). The horizontal sections are equipped with differential pressure transducer to measure the pressure drop inside the test section. At the end of the test section, an acrylic section of 20 cm allows the visible inspection of the flow behavior. After having passed the test section, the fluid can be directed to the phase separator where water and oil can be separated by gravity or alternatively to the cyclone whose outlet is connected to the phase separator. The sketch layout of the experiment is shown in Fig. 6.

The generated air-water two-phase flow is circulated through the flow loop using a vertical centrifugal pump that can provide a maximum flow rate of 40 l/min of water (see Fig. 7). On the other hand, the air is introduced to the system using a pressure regulator connected at the inlet of the compressed air; the air pressure in this step is measured by the equipment in Fig. 8. The flow rate of the water is measured using an electromagnetic flow meter and an accurate pressure transducer is used to measure the differential pressure drop over 1.5 mb long and mounted about 3.5 mb downstream the mixing section (see the device in Fig. 9).

The data acquisition procedure is carried out for better and more accurate data gathering; we used the machine in Fig. 10 for this purpose. We targeted a group of the experimental observations at 25 °C, 54 different measurements of Q and ΔP have been collected, and

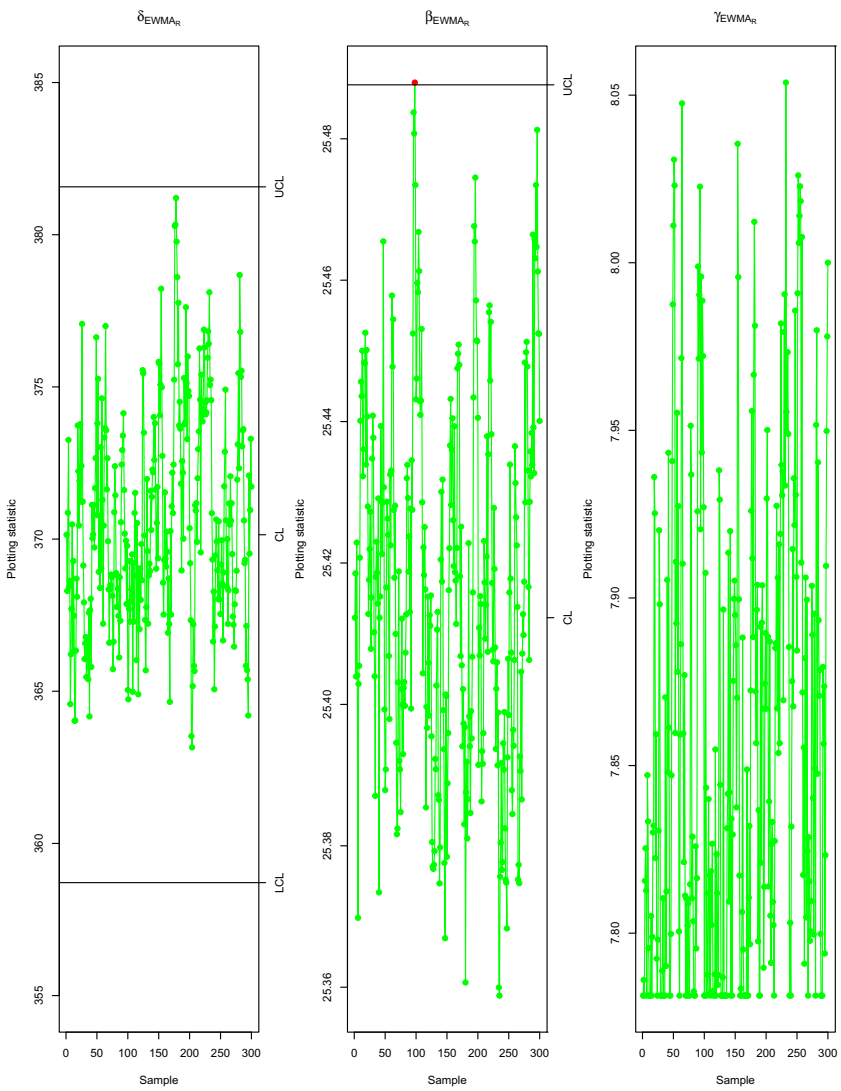

Fig. 11 EWMA_3 chart for monitoring two-phase flow

preliminary investigations have been conducted on the gathered data. There exist 18 levels of the volume flow rate (in liter/min) that equal 2.5, 3.8, 5.6, 7.2, 8.9, 10.6, 12.3, 13.9, 18.6, 20.3, 22.3, 24.0, 21.4, 22.2, 23.1, 24.3, 25.7, and 26.7. In the stated study, we consider the difference of pressure in two point (ΔP) as a dependent variable and the flow rate (Q) as an independent variable. We used an approach based on bootstrapping method similar to that been introduced by [25] and repeated the scenario for 10,000 iterations to extract the true parameters for our model.

The flow rate (Q) is direct proportion to the difference of pressure in two point (ΔP) and the model mathematically is represented as

$$\Delta P = -43.46 + 25.37 * Q \tag{21}$$

The model in Eq. 21 is considered as a reference to the relationship between the flow rate (Q) and the difference of pressure in two point (ΔP) with an estimated value of σ to equal 48.9.

7.4 Implementation of $EWMA_R$ and $EWMA_{PT}$ charts

To monitor the flow rate (Q) as it is a direct proportion to the difference of pressure in two point (ΔP), after we estimated the model in Eq. 21, we proceed with the following steps:

- From the bootstrapping, we found the value of the distrust constant $d = 0.0524$.
- We transformed the flow rate (Q) into $Q' = (Q - \bar{Q})$.
- We fixed $\lambda = 0.2$, $\text{ARL}_0 = 200$ with associated values of L given in Table 2.
- For the diagnosis purpose, the plotting statistics were plotted against the control limits given in Table 3.

Findings of diagnose have been plotted in Figs. 11, 12, and 13. It is clear from these figures that results assure our findings in the simulation study. We figure out the following outputs:

- For the intercept parameter, there is no significant improvement under different estimation strategies

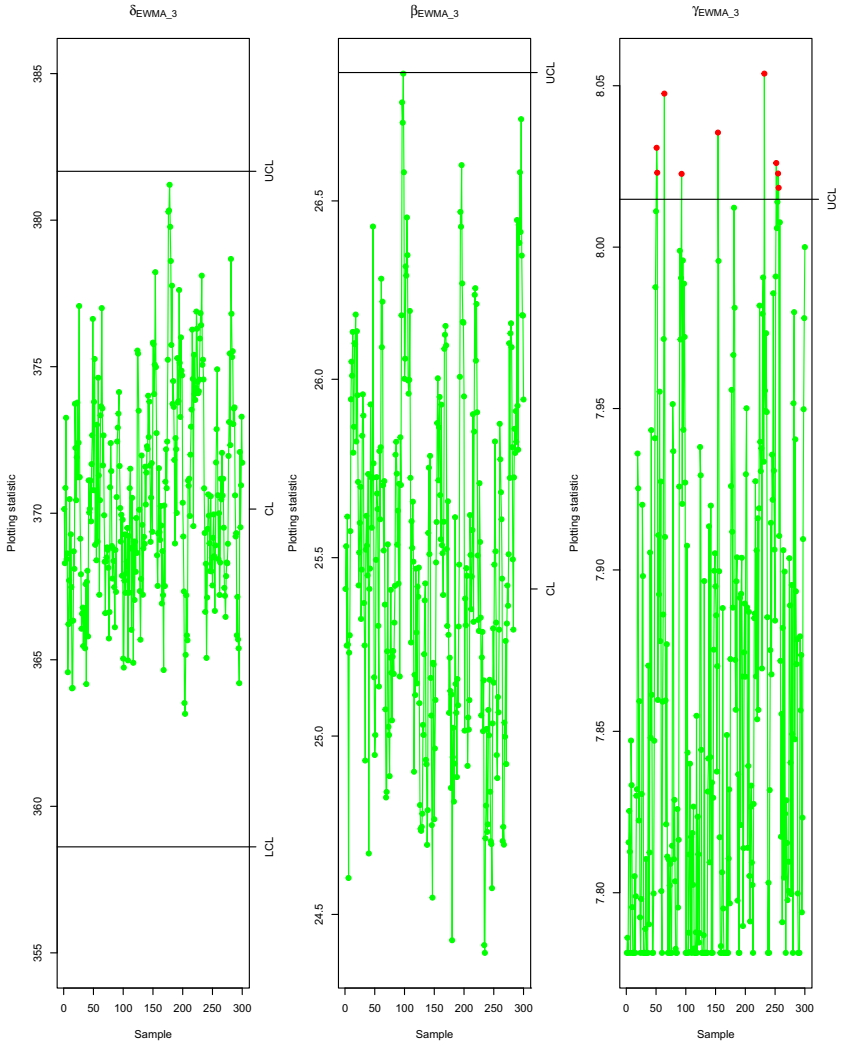

Fig. 12 $EWMA_R$ chart for monitoring two-phase flow

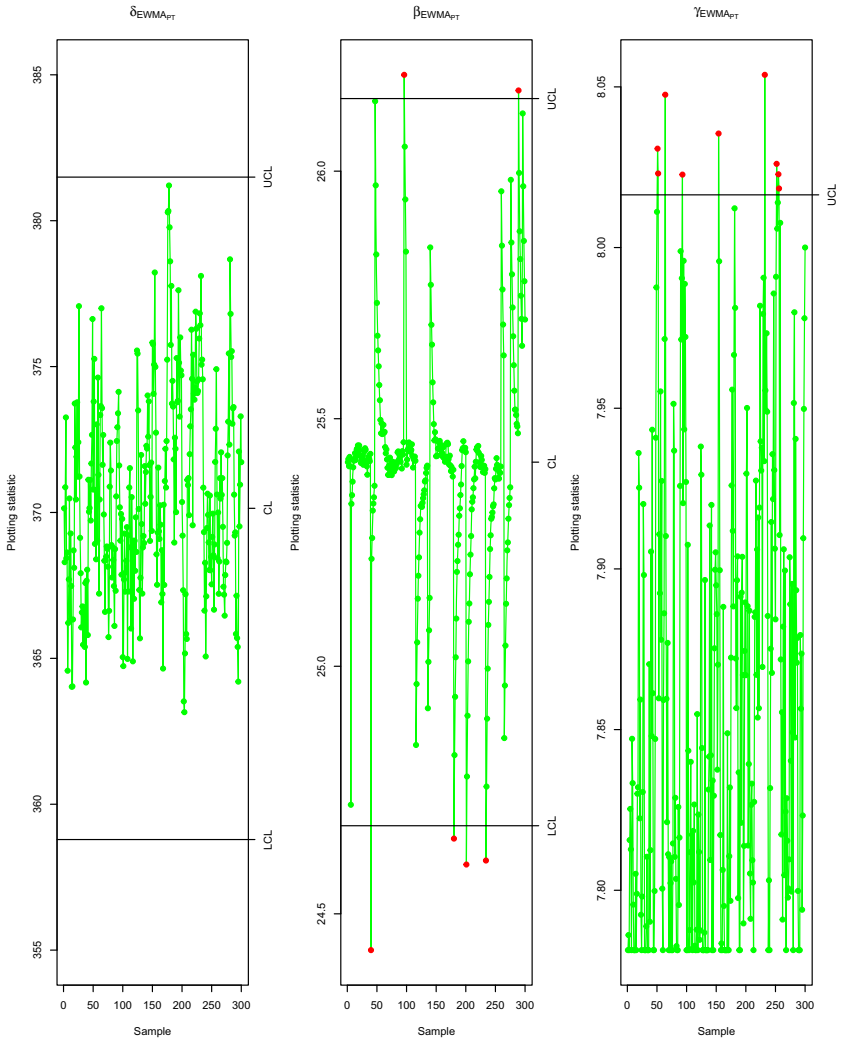

Fig. 13 $EWMA_{PT}$ chart for monitoring two-phase flow

because we standardized the explanatory variable. All the control charts failed to declare any out of control signal for the shifts in the process intercept.

- For the slope parameter, it is clear that $EWMA_{PT}$ excelled EWMA_3 and $EWMA_R$ to detect the shift in the fluid's pressure difference (ΔP) regarding the associate changes in the flow rate. The results matched what was concluded in the analytical and simulated results when $\Delta^2 > 0$.
- Regarding the error variance, it is clear that $EWMA_{PT}$ and $EWMA_R$ excelled EWMA_3 to detect the shift in the fluid's pressure difference (ΔP) regarding the associate changes in the flow rate.

8 Conclusions

An innovative scheme EWMA_3 was proposed for simultaneous monitoring of shifts in the parameters of a linear profile including the intercept, the slope, and the error variance of the process. In this study, we proposed new control charts by using new estimation strategies restricted estimator and pretest estimator.

The results showed that

- The $EWMA_R$ control chart outperforms all the other control charts under the different values of shifts in the slope and the error variance of the considered linear profile.
- The three control charts performed similarly under the shifts of the linear profile that was due to the useless of the UPI that caused by the adjusted exclamatory variable.
- Based on our numerical study, a bootstrapping method can be used to find the degree of distrust (d) in the null hypothesis. We observed that d has a significant impact on the performance of all estimates.

Overall, $EWMA_R$ performs performed better under the smaller values of d and small shifts, whereas $EWMA_{PT}$ with the smaller values of d was the worse. Under the larger values of d, $EWMA_R$ and $EWMA_{PT}$ approach to EWMA_3 and they perform similarly when $d = 0$.

Acknowledgments The authors would like to thank King Fahd University of Petroleum and Minerals (KFUPM) for providing excellent research facilities. The author Saddam Akber Abbasi would like to acknowledge Qatar University for providing excellent research facilities. The authors also thank the referees for their comments.

References

1. Agrawal R, Lawless JF (1999) Analysis of variation transmission in manufacturing processes–part II. J Qual
2. Lawless JF, Mackay RJ (1999) Analysis of variation transmission in manufacturing processes–Part I. J Qual
3. Kang L, Albin S (2000) On-line monitoring when the process yields a linear. J Qual Technol 32(4):418–426
4. Stover FS, Brill RV (1998) Statistical quality control applied to ion chromatography calibrations. J Chromatogr A 804(1-2):37–43. ISSN 00219673. https://doi.org/10.1016/S0021-9673(98)00094-6
5. Shewhart WA (1931) Economic control of quality of manufactured product. ASQ Quality Press
6. Roberts SW (1959) Control chart tests based on geometric moving averages. Technometrics 1(3):239–250
7. Page ES (1954) Continuous inspection schemes. Biometrika 41(1/2):100–115
8. Mahmoud MA, Woodall WH (2004) Phase I analysis of linear profiles with calibration applications. Technometrics 46(4):380–391. ISSN 0040-1706. https://doi.org/10.1198/004017004000000455
9. Noorossana R, Eyvazian M, Vaghefi A (2010) Phase II monitoring of multivariate simple linear profiles. Comput Ind Eng 58(4):563–570. ISSN 03608352. https://doi.org/10.1016/j.cie.2009.12.003
10. Dc Montgomery (2009) Introduction to statistical quality control. ISBN 9780470169926. https://doi.org/10.1002/1521-3773(20010316)40:6<9823::AID-ANIE9823>3.3.CO;2-C
11. Kim K, Mahmoud M, Woodall W (2003) ASQ: On the monitoring of linear profiles. J Qual Technol 35(3):317–328. ISSN 0361-0926. https://doi.org/10.1080/03610920701653136
12. Gupta S, Montgomery DC, Woodall WH (2006) Performance evaluation of two methods for online monitoring of linear calibration profiles. Int J Prod Res 44(10):1927–1942. ISSN 0020-7543. https://doi.org/10.1080/00207540500409855
13. Crowder SV, Hamilton MD (1992) An EWMA for monitoring a process standard deviation. J Qual Technol 24(1):12–21. ISSN 0022-4065
14. Ding D, Tsung F, Li J (2017) Ordinal profile monitoring with random explanatory variables. Int J Prod Res 55(3):736–749. ISSN 0020-7543. https://doi.org/10.1080/00207543.2016.1204476
15. Bancroft TA (1944) On biases in estimation due to the use of preliminary tests of significance. Ann Math Stat 15(2):190–204. https://doi.org/10.1214/aoms/1177731284
16. Stein C (1956) Inadmissibility of the usual estimator for the mean of a multivariate normal distribution *Proceedings* of the Third Berkeley symposium on ...
17. Ehsanes Saleh AKMd (2006) Theory of preliminary test and Stein-type estimation with applications: Theory of preliminary test and Stein-type estimation with applications, vol 102. Wiley, Hoboken. ISBN 9780471563754. https://doi.org/10.1198/jasa.2007.s190
18. Khan S, Hoque Z (2002) Estimation of the slope parameter for linear regression model with uncertain prior information, vol 36
19. Khan S, Hoque Z, Saleh AKMdE (2005) Estimation of the intercept parameter for linear regression model with uncertain non-sample prior information. Stat Pap 46(3):379–395. ISSN 0932-5026. https://doi.org/10.1007/BF02762840
20. Neter J, Kutner MH, Nachtsheim CJ, Wasserman W (1996) Applied linear statistical models, vol 4, Irwin, Chicago
21. Lawless JF (2002) Statistical models and methods for lifetime data. ISBN 0471372153
22. Steiner Stefan H (1999) EWMA control charts with time-varying control limits and fast initial response. J Qual Technol 31(1):75. ISSN 00224065
23. Darcy H (1856) Les fontaines publique de la ville de dijon. Dalmont, Paris, p 647
24. Soo SL, Stukel JJ, Martin Hughes J (1969) Measurement of mass flow and density of aerosols in transport. Environ Sci Technol 3(4):386–393
25. David A et al (1981) Freedman bootstrapping regression models. The Annals of Statistics 9(6):1218–1228